Shock Tube and Modeling Study of the Ignition of Propane

Kilyoung Kim and Kuan Soo Shin*

Department of Chemistry, Soongsil University, Seoul 156-743, Korea
Received November 29, 2000

The ignition of propane was investigated behind reflected shock waves in the temperature range of 1350-1800 K and the pressure range of 0.75-1.57 bar. The ignition delay time was measured from the increase of pressure and OH emission in the C_3H_8-O_2-Ar system. The relationship between the ignition delay time and the concentrations of propane and oxygen was determined in the form of mass-action expression with an Arrhenius temperature dependence. The numerical calculations were also performed to elucidate the important steps in the reaction scheme of propane ignition using various reaction mechanisms. The ignition delay times calculated from the mechanism of Sung *et al.*[1] were in good agreement with the observed ones.

Keywords : Shock tube, Ignition, Propane, Mechanism.

Introduction

Propane is the simplest hydrocarbon as practical hydrocarbon fuel and jet fuel and its thermochemical and combustion properties are closer to those of more complex fuels than light hydrocarbons like methane and ethane. Therefore, for wide application in practical life in terms of energy, economy, and environment, there have been many experiments and modeling studies on propane combustion.[1-15] The high temperature pyrolysis of propane has been investigated by Lifshitz *et al.*,[2] Koike *et al.*,[3] Chiang *et al.*,[4] and Al-Alami *et al.*[5] using various shock tube techniques. Propane oxidation behind shock waves, however, was not much studied experimentally except by Burcat *et al.*,[6] Hidaka *et al.*,[7] and Qin.[8] Burcat *et al.*[6] measured the ignition delay times of propane mixtures behind shock waves and reported the relationship between induction time and concentration of mixtures. Hidaka *et al.*[7] studied the oxidation of propane by observing the time variation of oxygen concentration using a quadrupole mass spectrometer-shock tube system. Qin[8] also studied the oxidation of propane behind the reflected shock waves by measuring OH absorption profiles using narrow line width cw ring dye laser. Warnatz[9] conducted the experiments on laminar flames and a turbulent flow reactor, and Cathonnet *et al.*[10] on a quartz flow reactor. Recently, Sung *et al.*[1] studied the structure of counterflow CH_4/N_2 and C_3H_8/N_2 diffusion flames. They measured concentration profiles of major species with spontaneous Raman scattering and computationally simulated with detailed kinetics and transport.

The detailed chemical reaction mechanisms of propane combustion were presented by Westbrook *et al.*,[11] Jachimowski,[12] Dagaut *et al.*,[13] and Sloane.[14] The reaction mechanisms of propane oxidation in the early literature considered only limited numbers of chemical intermediates. In Jachimowski's mechanism,[12] C_3H_4 species were not included at all. Westbrook *et al.*[11] and Sloane[14] included C_3H_5 and C_3H_4 but did not include separate reactions for different C_3H_5 and C_3H_4 isomers. Dagaut *et al.*[15] gave a more complete mechanism, including almost all C_3 isomer species. In order to understand the detailed oxidation of propane including rich conditions, however, hydrocarbon species larger than C_4 should be included in the mechanism.

The aim of the present study is to elucidate the rate determining steps in the reaction scheme of propane oxidation during the ignition period, and to deduce an analytical expression for the calculations over wide range of experimental conditions. For this purpose, experiments on the ignition of nine different C_3H_8-O_2-Ar mixtures in the temperature range of 1350-1800 K, and numerical modeling of the ignition process, have been carried out.

Experimental Section

The experiments were performed behind reflected shock waves in stainless-steel shock tube which was described in detailed elsewhere.[16,17] The apparatus consists of a 514 cm (6.02 cm i.d.) 304 stainless-steel tube separated from the He driver gas chamber by an unscored aluminium diaphragm with 0.1 mm thickness. The tube is routinely pumped between experiments to $< 10^{-7}$ torr by turbo molecular pump (Varian, 969-9002) system. The velocity of shock wave was measured with 5 pressure transducers (PCB 113A21) mounted along the end portion of the shock tube, and the temperature and the density in the reflected shock wave regime were calculated from this velocity. This procedure has been explained in our previous paper[16] and the corrections for boundary-layer perturbation were applied.[18]

The ignition was measured by the sudden increase of pressure profile and OH emission intensity. The pressure measurements were made using a pressure transducer (PCB 113A21) which was located at 1.0 cm from the reflecting surface. The characteristic ultraviolet emission from OH radical species at 306.7 nm was monitored using a photomultiplier tube (ARC DA-781) with a band path filter (Andower, 308 nm) through the sapphire window which was mounted flush at 1.0 cm from the end plate of the shock tube. The window was masked with 1 mm width slit in order to reduce emission intensity and to improve the time resolu-

Table 1. The experimental conditions of C_3H_8-O_2-Ar mixtures

	Compositions of mixtures (%)			equivalence ratio (Φ)	τ (μsec)	T_5 (K)	P_5 (atm)
	C_3H_8	O_2	Ar				
Mixture 1	2.0	10.0	88.0	1	43-726	1397-1570	0.94-1.14
Mixture 2	4.0	10.0	86.0	2	49-1370	1412-1673	1.16-1.57
Mixture 3	2.0	5.0	93.0	2	50-459	1506-1713	0.99-1.25
Mixture 4	1.0	5.0	94.0	1	53-549	1436-1622	0.81-0.99
Mixture 5	1.6	8.0	90.4	1	59-978	1396-1558	0.87-1.04
Mixture 6	1.6	4.0	94.4	2	48-906	1494-1760	0.93-1.24
Mixture 7	0.8	8.0	91.2	0.5	68-1038	1357-1506	0.75-0.89
Mixture 8	1.0	7.5	91.5	0.75	39-1460	1350-1566	0.75-0.96
Mixture 9	2.0	20.0	78.0	0.5	64-1250	1315-1499	0.93-1.18

tion of the system. Both the pressure and the OH emission traces were fed into a digital oscilloscope (HP 45601A).

The compositions of the nine different mixtures are given in Table 1. The equivalence ratio was varied from 0.5 to 2.0 to examine the composition dependences on the ignition delay time. C_3H_8 (99.5%, Dongmin), O_2 (99.99%, Dongmin) and Ar (99.9993%, Donga) were used without further purification. He (99.9995%, Dongmin) was used as a driver gas. Test gas mixtures were prepared manometrically and then used after keeping for over 24 hours in aluminium cylinders. The initial pressure (P_1) was fixed to 20 torr and the shock velocity was controlled by changing the pressure of He driver gas. The measurements covered a temperature range (T_5) of 1350-1800 K and a pressure range (P_5) of 0.75-1.57 bar behind reflected shock waves. The measured ignition delay time ranged from 39 to 1370 μs.

Results and Discussion

Figure 1 shows a typical oscilloscope trace for pressure and OH emission profiles measured at 1.0 cm from the reflecting end plate. The upper trace records the total pressure and the lower trace the OH emission. The ignition delay time (τ) was defined as the time interval between the arrival

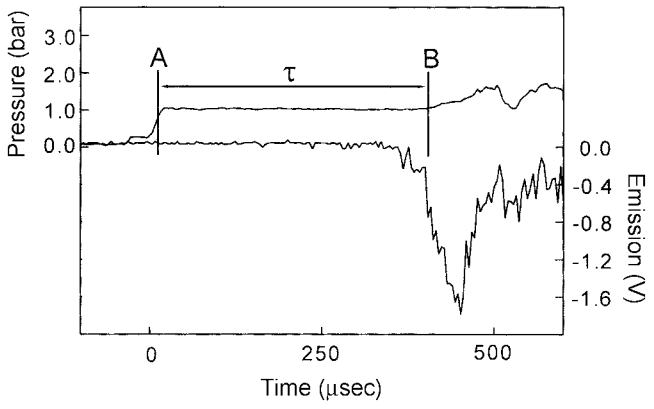

Figure 1. Typical experimental record showing pressure (upper) and OH emission (lower). Experimental conditions were P_1=20 torr, P_5 =0.97 bar, and T_5=1430 K in mixture 1. (A: an arrival of a reflected shock wave; B: onset of the ignition; τ: ignition delay time).

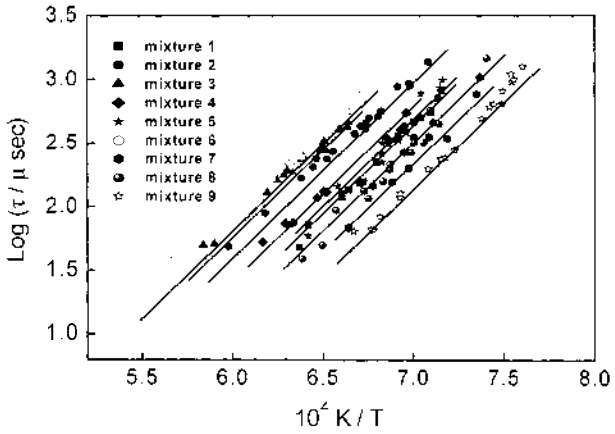

Figure 2. Ignition delay times for the mixtures shown in Table 1. Lines represent the least squares fits for the corresponding mixtures using the expression in the text.

of the reflected shock wave front and the onset of an ignition. The ignition delay time derived from the OH emission is almost the same as that derived from the pressure profile.

The effects of propane and oxygen concentrations on the ignition delay are shown in Figure 2. A correlation between ignition delay and concentration was customarily summarized in the form of mass-action expression with an Arrhenius temperature dependence.[19] Multiple regression analysis was employed to obtain the best-fit parameters. This procedure gave

$$\tau = 4.5 \times 10^{-14} \exp(61.9 \text{ kcal mol}^{-1}/RT) \; [C_3H_8]^{1.22} \; [O_2]^{-1.61} \; (\text{mol/cm}^3)^{0.39} \text{ sec}$$

where the ignition delay time τ and the concentration are given in sec and mol/cm^3, respectively. The reliability of this empirical formula was tested by plotting all data as $\log(\tau / \{[C_3H_8]^{1.22}[O_2]^{-1.61}(\text{mol/cm}^3)^{0.39}\text{sec}\})$ *vs.* $10^4/T$. As shown in Figure 3, all points lie close to a single line. The power dependence of propane indicates self-inhibiting effect; the ignition delay time increases by increasing the concentration of propane. On the other hand, the power dependence of oxygen indicates the promotion effect: the ignition delay

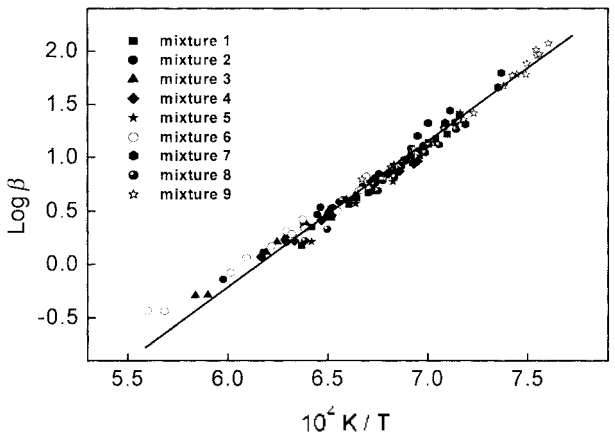

Figure 3. A plot of $\log(\tau / \{[C_3H_8]^{1.22}[O_2]^{-1.61}(\text{mol/cm}^3)^{0.39}\text{sec}\})$ *vs.* $10^4/T$ for all mixtures; $\beta = \tau / \{[C_3H_8]^{1.22}[O_2]^{-1.61}(\text{mol/cm}^3)^{0.39}\text{sec}\}$.

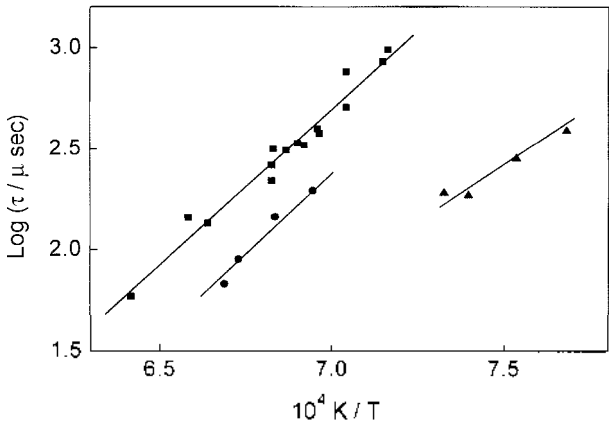

Figure 4. The effect of initial pressure (P_1) on ignition delays at 20, 55, and 220 torr in 1.6% C_3H_8-8.0% O_2-90.4% Ar mixture. Symbols are for: ■ (P_1=20 torr) from this work, ● (P_1=55 torr) from Ref. 6, and ▲ (P_1=220 torr) from Ref. 6.

time decreases with increasing the concentration of oxygen. In this investigation, the argon dependence on the ignition of propane was not tried to obtain because the concentration of argon in our mixtures was not varied much. Burcat *et al.*[6] also found no argon dependence on the ignition of propane in their experimental conditions.

It is, however, worth noting that the parameters are valid only for the specific ranges of pressure, temperature, and concentration over which the ignition delays were measured. As a result, any attempt to use such formula to describe experimental data obtained under different conditions may give quite considerable deviations from measured values. Burcat *et al.*[6] reported ignition delay time for 1.6% C_3H_8 - 8.0% O_2-90.4% Ar mixture at the initial pressure (P_1) of 55 and 220 torr. In this study, ignition delays of the same composition of the mixture (mixture 5 in Table 1) with different initial pressure (P_1), 20 torr, were measured. Figure 4 shows the comparison of our results with those of Burcat *et al.*[6] and also shows the effect of initial pressure (P_1) on the ignition delay of propane at 20 torr (from this study), 55 torr (from Burcat *et al.*[6]), and 220 torr (from Burcat *et al.*[6]) in 1.6% C_3H_8-8.0% O_2-90.4% Ar mixture. As the initial pressure of the gas mixtures increases, the ignition delay time decreases significantly. This initial pressure effect can be rationalized by the propane decomposition reaction, $C_3H_8 (+ M) \rightarrow C_3H_7 + H (+ M)$, which is pressure dependent.

The modeling study of the ignition of propane was also performed using the propane oxidation mechanisms of Sung *et al.*,[1] Qin,[8] Westbrook *et al.*,[11] Jachimoski,[12] Dagaut *et al.*,[13] Glassman,[20] Konnov,[21] and GRI 3.0.[22] Computations of modeling were carried out using Sandia Chemkin III code.[23] Thermodynamic data were obtained from GRI 3.0 version thermodynamics[22] and Chemkin thermodynamic data base.[24] The rate constants for the reverse reactions were calculated from the forward rate constants and the appropriate equilibrium constants. As shown in Figure 5, the observed results are in good agreement with the calculated ones using the mechanisms of Sung *et al.*,[1] Glassman,[20] and Konnov,[21] among them. The calculated ignition delay times using the mechanism of Sung *et al.*,[1] which consists of 621 reactions with 92 species, shows the best agreement with the observed ones for all mixtures.

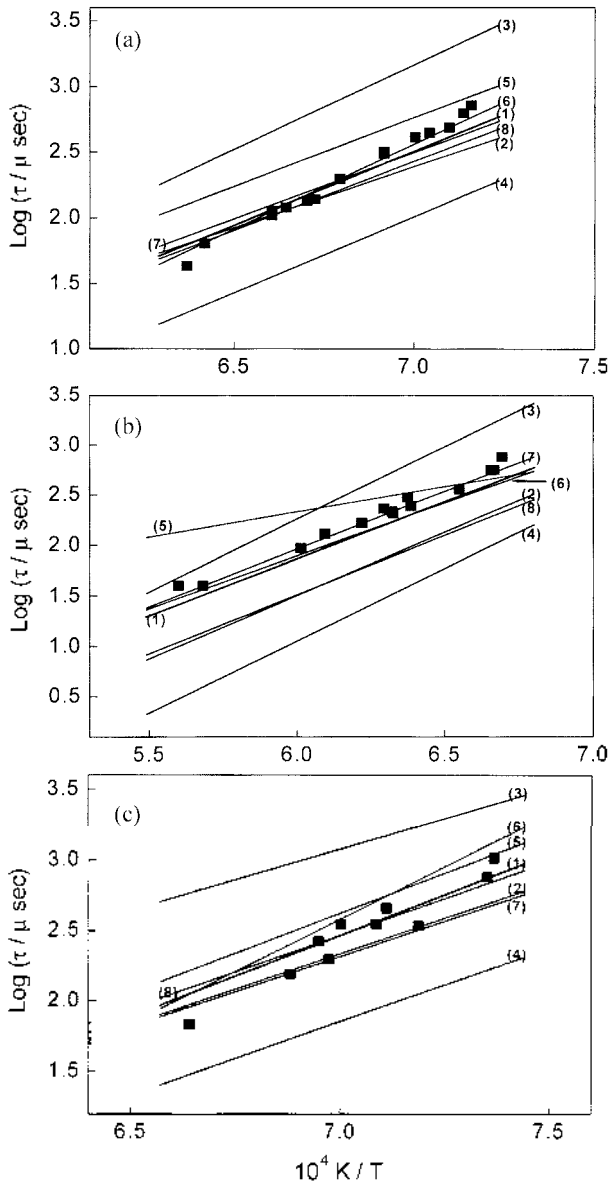

Figure 5. Comparison of observed ignition delay times (symbols) with calculated ones (lines). (a) mixture 1 (stoichiometric); (b) mixture 6 (rich); (c) mixture 7 (lean). Lines are for: (1) Sung *et al.*[1]; (2) Qin[8]; (3) Westbrook *et al.*[11]; (4) Jachimoski[12]; (5) Dagaut *et al.*[13]; (6) Glassman[20]; (7) Konnov[21]; (8) GRI 3.0,[22] respectively.

In the complex reaction mechanism, all of elementary reactions do not contribute equally to the ignition delay time of propane, but some of them may do essentially. In order to find the sensitive reactions, logarithmic sensitivity analysis,[25] listed in Table 2, was performed using the mechanism of Sung *et al.*[1] The flow analysis,[26] shown in Figure 6, was also carried out by calculating the net reaction rates. From these sensitivity and flow analyses, the reaction scheme of the ignition process of propane was obtained.

$$C_3H_8 (+ M) \rightarrow C_2H_5 + CH_3 (+ M) \quad (1)$$

Table 2. Logarithmic sensitivity values of ignition delay time for mixtures 1 (stoichiometric), 6 (rich), and 7 (lean) at T_5=1492 K. Sensitivities less than 0.01 are not listed

Reaction	Sensitivity (S_n)		
	Mixture 1	Mixture 6	Mixture 7
$C_3H_8 + H \rightarrow n\text{-}C_3H_7 + H_2$	0.27	-0.01	0.23
$C_3H_8 + H \rightarrow i\text{-}C_3H_7 + H_2$	0.20	0.27	0.20
$C_3H_8 + OH \rightarrow i\text{-}C_3H_7 + H_2O$	0.05	-0.03	-0.01
$C_2H_5 + CH_3(+M) \rightarrow C_3H_8(+M)$	-0.19	-0.14	-0.11
$C_3H_6 + H \rightarrow a\text{-}C_3H_5 + H_2$	0.16	0.22	0.17
$C_3H_6 + OH \rightarrow a\text{-}C_3H_5 + H_2O$	0.21	0.12	0.20
$a\text{-}C_3H_5 + HO_2 \rightarrow OH + C_2H_3 + CH_2O$	-0.13	-0.07	-0.01
$C_2H_4 + OH \rightarrow C_2H_3 + CH_2O$	-0.14	-0.04	-0.01
$C_2H_4 + H \rightarrow C_2H_3 + H_2$	-0.13	-0.07	0.00
$CH_3 + CH_3(+M) \rightarrow C_2H_6(+M)$	0.06	0.03	0.05
$CH_3 + HO_2 \rightarrow CH_3O + OH$	-0.19	-0.08	-0.07
$CH_3 + OH \rightarrow CH_2^* + H_2O$	-0.29	-0.26	-0.26
$CH_2^* + O_2 \rightarrow CO + H_2O$	0.05	0.01	0.14
$HO_2 + OH \rightarrow O_2 + H_2O$	0.16	0.04	0.21
$H + O_2 \rightarrow O + OH$	-0.89	-1.11	-0.92

This is the important initiation reaction in the oxidation of propane at high temperature. The propane decomposes into C_2H_5 and CH_3 rather than to C_3H_7 and H because the dissociation energy of C-C bond is weaker than that of C-H bond. Once C_2H_5 is formed, C_2H_5 radical rapidly splits into more stable C_2H_4 and H.

$$C_2H_5 (+ M) \rightarrow C_2H_4 + H (+ M) \quad (2)$$

H atoms generated through the decomposition of C_2H_5 radicals attack C_3H_8 to produce propyl radicals (C_3H_7) and H_2, which are the main fuel-consumption reactions.

$$C_3H_8 + H \rightarrow n\text{-}C_3H_7 + H_2 \quad (3)$$
$$C_3H_8 + H \rightarrow i\text{-}C_3H_7 + H_2 \quad (4)$$

H atoms also react with O_2 molecules and produce O and OH.

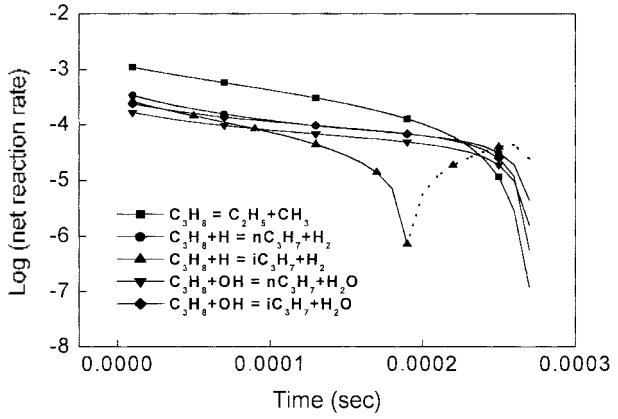

Figure 6. Net reaction rates of propane consumption reactions in mixture 1 at T_5=1456 K; The solid lines indicate that the net reaction proceeds in the forward direction; the dotted lines indicate the reverse direction.

$$H + O_2 \rightarrow O + OH \quad (5)$$

Reaction (5) is the most important chain-branching reaction in all hydrocarbon combustion, which accelerates the overall oxidation rate. Because of this reaction, the ignition delay time decreased with increasing the concentration of O_2. The ignition delay time, however, increased with increasing the concentration of C_3H_8. Reactions (3) and (4) decelerates the overall ignition rate, because C_3H_8 can compete with O_2 on the reactions with H atoms. The same phenomena were observed in the oxidation mechanism of methane[16] and ethane.[27] The O and OH chain-carriers produced through reaction (5) react with the fuel, C_3H_8, and generate propyl radicals.

$$C_3H_8 + O \rightarrow C_3H_7 + OH \quad (6)$$
$$C_3H_8 + OH \rightarrow C_3H_7 + H_2O \quad (7)$$

Two different types of propyl radicals, n-C_3H_7 and i-C_3H_7, are considered in this study. Normal propyl radicals are rapidly decomposed to methyl radicals and ethylene.

$$n\text{-}C_3H_7 \rightarrow CH_3 + C_2H_4 \quad (8)$$

while the majority of the iso-propyl radicals produce H atoms and propylene.

$$i\text{-}C_3H_7 \rightarrow H + C_3H_6 \quad (9)$$

Propyl radicals decompose according to the β-scission rule,[20] which implies that the bond that will break is one position removed from the radical site. Normally, reaction (8) tends to retard the overall process of fuel consumption, while reaction (9) tends to accelerate this process. Our calculation shows that the net reaction rate of reaction (8) is about 10 times higher than that of reaction (9) during the whole ignition delay. Once C_3H_6 is formed, C_3H_6 reacts with H and OH to produce allyl radicals (a-C_3H_5), which are the main sources of C_3H_6 consumption.

$$C_3H_6 + H \rightarrow a\text{-}C_3H_5 + H_2 \quad (10)$$
$$C_3H_6 + OH \rightarrow a\text{-}C_3H_5 + H_2O \quad (11)$$

Figure 7 shows the calculated concentration profiles of stable intermediates. C_2H_4 is formed from C_2H_5 dissociation

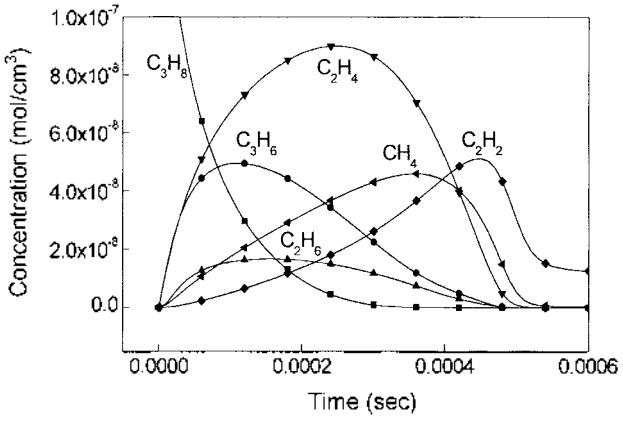

Figure 7. Calculated concentration profiles of C_3H_8, C_3H_6, C_2H_6, C_2H_4, CH_4, and C_2H_2 at T_5=1401 K, P_5=1.0 bar in mixture 1.

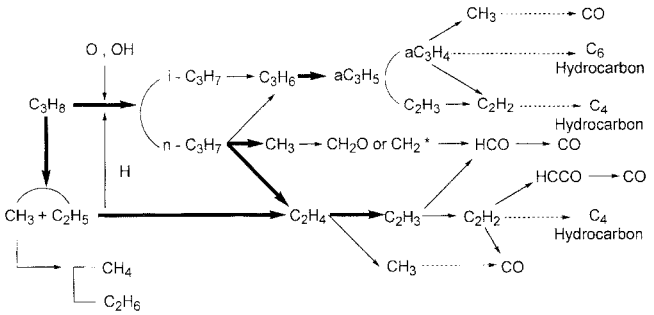

Scheme 1. Reaction scheme of the ignition of propane. The thick lines indicate that the channel deeply affects in overall ignition process and the dotted lines show that the channels are omitted in the midway.

or C_3H_7 decomposition. The reaction of C_2H_4 with the H and OH are the main sources of C_2H_3 formation. C_2H_2 can be generated from the reactions of C_2H_3 with H, O, and OH radicals. Ethylene and acetylene are known as important intermediates in the formation of soot.[28] In order to understand more details of the propane oxidation, especially in the propane rich mixtures, the soot formation sub-mechanism should be included in the whole propane oxidation mechanism. Therefore, it is necessary to perform more experimental and modeling studies on the alkene and alkyne oxidations at combustion temperatures. Scheme 1 represents the propane ignition mechanism schematically.

Conclusions

In the present study, a comprehensive shock tube and modeling investigation was performed on the ignition of C_3H_8-O_2-Ar mixtures in the temperature range of 1350-1800 K and the pressure range of 0.75-1.57 bar. The ignition delay times were measured from the increase of the pressure and the OH emission. A correlation between ignition delay time and concentrations of propane and oxygen could be summarized in the following empirical formula.

$$\tau = 4.5 \times 10^{-14} \exp(61.9 \text{ kcal mol}^{-1}/RT) [C_3H_8]^{1.22} [O_2]^{-1.61} (\text{mol/cm}^3)^{0.39} \text{sec}$$

The numerical calculations were also performed to elucidate the important steps in the reaction scheme of propane ignition using various reaction mechanisms. It was found that the ignition delay times calculated from the mechanism of Sung *et al.*[1] were in good agreement with the experimental data. Reaction pathways leading to propane ignition were identified and discussed.

Acknowledgment. This work was supported by Korea Research Foundation Grant (KRF-99-015-DI0050).

References

1. Sung, C. J.; Li, B.; Wang, H.; Law, C. K. *27th Symp. (Int.) on Combustion*; The Combustion Institute: Pittsburgh, 1998; p 1523.
2. Lifshitz, A.; Frenklach, M. *J. Phys. Chem.* **1975**, *79*, 686.
3. Koike, T.; Gardiner, W. C. *J. Phys. Chem.* **1980**, *84*, 2005.
4. Chiang, C.; Skinner, G. B. *18th Symp. (Int.) on Combustion*; The Combustion Institute: Pittsburgh, 1981; p 915.
5. Al-Alami, M. Z.; Klefer, J. H. *J. Phys. Chem.* **1983**, *87*, 499.
6. Burcat, A.; Lifshitz, A.; Sheller, K.; Skinner, G. B. *13th Symp. (Int.) on Combustion*; The Combustion Institute: Pittsburgh, 1971; p 745.
7. Hidaka, Y.; Ikoma, A.; Kawano, H.; Suga, M. *Int. J. Mass Spec. Ion Phys.* **1983**, *48*, 71.
8. Qin, Z. *Ph. D. Dissertation*; University of Texas at Austin: 1998.
9. Warnatz, J. *Combust. Sci. Tech.* **1983**, *34*, 177.
10. Cathonnet, M.; Boettner, J. C.; James, H. *18th Symp. (Int.) on Combustion*; The Combustion Institute: Pittsburgh, 1981; p 903.
11. Westbrook, C. K.; Pitz, W. J.; Urtiew, P. A. Lawrense Livermore National Laboratory: UCRL-88943, 1983.
12. Jachimowski, C. J. *Combust. Flame* **1984**, *55*, 213.
13. Dagaut, P.; Cathonnet, M.; Boettner, J. C.; Gaillard, F. *Combust. Sci. Tech.* **1987**, *56*, 23.
14. Sloane, T. M. *Combust. Sci. Tech.* **1992**, *83*, 77.
15. Dagaut, P.; Cathonnet, M.; Boettner, J. C. *Int. J. Chem. Kinetics* **1992**, *24*, 813.
16. Jee, S. B.; Kim, W. K.; Shin, K. S. *J. Korean Chem. Soc.* **1999**, *43*, 156.
17. Jee, S. B.; Kim, K.; Shin, K. S. *Bull. Korean Chem. Soc.* **2000**, *21*, 1015.
18. Kim, W. K.; Shin, K. S. *J. Korean Chem. Soc.* **1997**, *41*, 600.
19. Tsang, W.; Lifshitz, A. *Annu. Rev. Phys. Chem.* **1990**, *41*, 559.
20. Glassman, I. *Combustion*, 3rd Ed.; Academic Press: San Diego, 1996.
21. Konnov, A. A. *Detailed Reaction Mechanism for small hydrocarbons Combustion*; Release 0.4, http://homepage.vub.ac.be/~akonnov/, 1998.
22. GRI-Mechanism 3.0 is available by World Wide Web using the URL locator http://euler.berkeley.edu/gri_mech/version30/text30.html/, 1999.
23. Kee, R. J.; Rupley, F. M.; Meeks, E.; Miller, J. A. *Chemkin-III: A Fortran Chemical Kinetics Package for the Analysis of Gas-Phase Chemical and Plasma Kinetics*; Sandia National Laboratories Report SAND96-8216; 1996.
24. Kee, R. J.; Rupley, F. M.; Miller, J. A. *The Chemkin Thermodynamic Data Base*; Sandia National Laboratories Report SAND87-8215B; 1990.
25. Gardiner, W. C. Jr. *J. Phys. Chem.* **1977**, *81*, 2367.
26. Lissianski, V. V.; Zamansky, V. M.; Gardiner, W. C., Jr. In *Gas-Phase Combustion Chemistry*; Gardiner, W. C., Jr., Ed.; Springer-Verlag: New York, 2000; p 1.
27. Shim, S. B.; Jeong, S. H.; Shin, K. S. *J. Korean Chem. Soc.* **1998**, *42*, 575.
28. Bastin, E.; Delfau, J. L.; Reuillon, M.; Vovelle, C.; Warnatz, J. *22nd Symp. (Int.) on Combustion*; The Combustion Institute: Pittsburgh, 1988; p 313.